2014

Experimental Analysis Of Twisted Shaped Spot Evaporators At High Heat Fluxes

Tobias Knipping
Karlsruhe UAS, Institute of Materials and Processes (IMP), Germany, tobias.knipping@hs-karlsruhe.de

Michael Arnemann
Karlsruhe UAS, Institute of refrigeration, air conditioning and environmental technology (IKKU), Germany, michael.arnemann@hs-karlsruhe.de

Ullrich Hesse
TU Dresden, BITZER Chair of Refrigeration-, Cryo- and Compressor Technology, Germany, ullrich.hesse@tu-dresden.de

Frank Humpfer
Karlsruhe UAS, Institute of Materials and Processes (IMP), Germany, frank.humpfer@hs-karlsruhe.de

Experimental analysis of twisted shaped spot evaporators at high heat fluxes

Tobias KNIPPING[1]*, Michael ARNEMANN[2], Ullrich HESSE[3], Frank HUMPFER[1]

[1]Karlsruhe UAS, Institute of Materials and Processes (IMP),
76133 Karlsruhe, Germany
tobias.knipping@hs-karlsruhe.de, phone: +49 (721) 925-2140

[2]Karlsruhe UAS, Institute of Refrigeration, Air Conditioning and Environmental Engineering (IKKU),
76133 Karlsruhe, Germany
michael.arnemann@hs-karlsruhe.de, phone: +49 (721) 925-1842

[3]TU Dresden, BITZER Chair of Refrigeration-, Cryo- and Compressor Technology
01069 Dresden, Germany
ullrich.hesse@tu-dresden.de, phone: +49 (351) 463-32548

* Corresponding Author

ABSTRACT

Devices for cooling high heat fluxes within small available spaces are called spot evaporators. Areas of application are for example the cooling of molds, power electronics or cutting tools in drilling processes. The functionality of the spot evaporator bases on its geometry and is a combination of spray-cooling and pipe flow. Spray-cooling or jet impingement cooling is able to achieve high heat fluxes even at overcritical wall temperatures. To reach the same effects within the pipe-flow part of the spot evaporator, this part has to be twisted shaped.

The paper focuses on the experimental analysis of the twisted shaped spot evaporator by varying fundamental parameters corresponding to the Model of Yagov. Two methods of generating the twist have been developed and compared to each other.

The experimental results will be discussed. They show that the averaged critical heat flux can be raised up to 30 % compared to spot evaporators without twisted flow. Refrigerant R404A is used.

1. INTRODUCTION

The cooling of high heat fluxes (up to 10^6 W/m² or more) is well known in the fields of power electronics or fusion power plants (Marcinichen *et al*., 2013; Milnes, 2010). Due to enhancements in modern production processes (Hong and Ding, 2001; Karaguezel *et al*., 2013) there is a great demand of thermal stability to achieve reproducible results. The challenge is that available spaces are process-related relatively small while thermal loads are relatively high. Examples are molding technologies, linear motion drives and milling tools for nickel-alloys.

Challenging effects within molding technology have been discussed by Knipping *et al*. (2012) in detail. The milling of nickel-alloys (i.e. Inconel 718) is currently in the focus of production-orientated research (Wessels, 2007; Mirghani *et al*., 2007; Pusavec *et al*., 2010). Two critical thermal material characteristics superpose each other when milling these materials. First the high ductility of Inconel which leads to high shear stress rates during the milling process (Weinert, 2005). Second the low thermal conductivity of the material (11.4 W/mK). The superposition of both leads to high amounts of heat energy which can't be discharged through the chips like in regular milling processes. Process heat is therefore discharged through the cutting tool, which leads to rapid thermal wear (Denkena and Toenshoff, 2011).

Nitrogen (R-728) or carbon dioxide (R-744) as refrigerant is used in latest research in the field of cryogenic cutting (Mirghani, 2007). The refrigerant is lead to the in-process cutting tool in fluid, relaxed state. To cool the tool, evaporation enthalpy of the refrigerant is used. Disadvantages of this system are both, the atomic diffusion process which leads to changes in the surface of work piece and cutting tool (Denkena and Toenshoff, 2011) and the open-loop cycle which leads to high process costs.

Linear motors are more and more used in building machine tools (Hein, 2009). Reasons are the high achievable acceleration (up to 100 m/s²), low friction rates due to missing mechanical transmission elements and good type of control (Ausderau, 2004). The main disadvantage is the limitation of the maximum load due to thermal reasons (Weck and Brecher, 2006). According to the quasi-linear relation between constructed space and maximum transferrable load there are actually only limited applications (Ganz, 2012). To solve this problem, linear motors are presently cooled with water to achieve higher power densities.

State of the art is the convective cooling of linear motors or with chillers. Ganz (2012) showed that cooling linear motors with refrigerants means enhancement of loads by factor 2.3 compared to a linear motor with convective cooling. Using the evaporation enthalpy the cooling of linear motors with refrigerants has advantages related to mass flows, flow cross sections and achievable heat flux coefficients. Boiling at high heat fluxes is limited by the critical heat flux. By reaching this point a vapor layer will be set up between the liquid phase of the refrigerant and the wall of the heat exchanger causing a loss of heat transfer due to bad heat transfer coefficients and a change of heat transfer mechanism (Leidenfrost-effect).

To cool high heat fluxes in small available spaces Knipping *et al.* (2012) developed a new evaporator called spot-evaporator (figure 1). Within these evaporators, refrigerant is led within concentric capillary tubes into a blind hole processed with deep hole drilling or drilling EDM-technology. This leads to split flow mechanisms as shown in figure 1. The front section could nearly be described as jet impingement cooling, the rear section as pipe flow. With jet impingement cooling high heat fluxes can be processed (Bogdanic, 2012). This leads to an effective cooling of high heat fluxes and high wall temperatures (Seiler-Marie *et al*., 2004). The pipe flow section of the spot evaporator can nearly be described as a heated pipe with internal cooling device. Critical heat fluxes can be calculated as described in VDI Wärmeatlas p. Hbc 1 (2013).

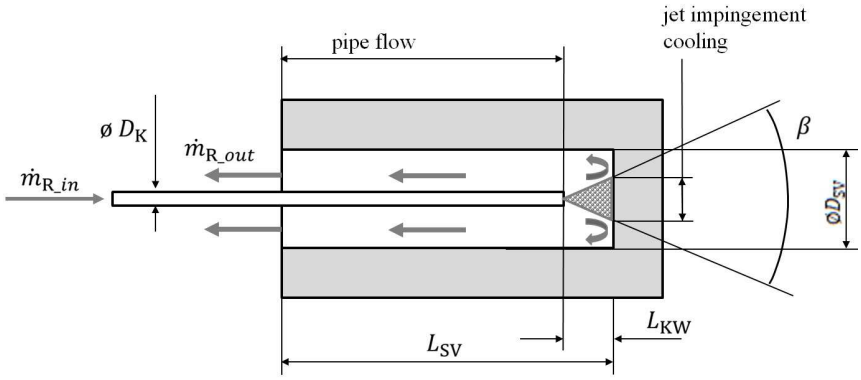

Figure 1: Layout of o spot-evaporator with incoming mass flow ($\dot{m}_{R\_in}$), outgoing mass flow ($\dot{m}_{R\_out}$), spraying angle β, length of spot evaporator (L_{SV}), diameter of the capillary tube ($\emptyset D_{SV}$) and distance between front surface and nozzle (L_{KW})

To enhance heat transfer rates in pipes several methods are described. A promising method to rise the critical heat flux in pipes is the generation of twisted flow (Chang *et al*., 2006). Several methods to generate twisted flow in pipes have been described by Webb (1994):

- twisted tapes,
- wire inserts,
- spirally internally ribbed tube.

All methods are equal in their ability to enhance critical heat fluxes compared to pipe flow without twist (Celata and Cumo, 1992). As refrigerant water with subcooling of 250 K has been used. No comparison to evaporating refrigerants has been made.

To measure the increase of critical heat flux within an ideal twisted flow Chang *et al*. (2006) use the radial acceleration a_r. By using gravitational acceleration g, a_r can be normalized to
p0

$$\frac{a_\mathrm{r}}{g} = \frac{{w_\mathrm{t}}^2}{R \cdot g} = \frac{{w_\mathrm{a}}^2}{R \cdot g \cdot \tan^2(\varphi)} \tag{1}$$

In this equation φ is the incline of flow, w_t the tangential and w_a the axial flow velocity. R is the diameter of the pipe as shown in figure 2. Yagov (1988) developed a model to describe the critical heat flux in pool boiling. Later on he expanded this model to describe the critical heat flux in twisted flow (Yagov, 2006). He assumes, that in twisted flow there are similar proportions related to the departure on nuclear boiling at the pipe wall than in pool boiling. Yagov replaces the gravitational acceleration in his pool boiling model with the radial acceleration of the twisted flow. The radial acceleration forces a full wetting of the inner pipe wall, so annual flow can be assumed. As initial state a fully wetted wall, which means annular flow, is assumed. The influence of higher flow velocities, which means turbulent flow, remains unattended. Without twist generation annual flow could not be assumed at all states.

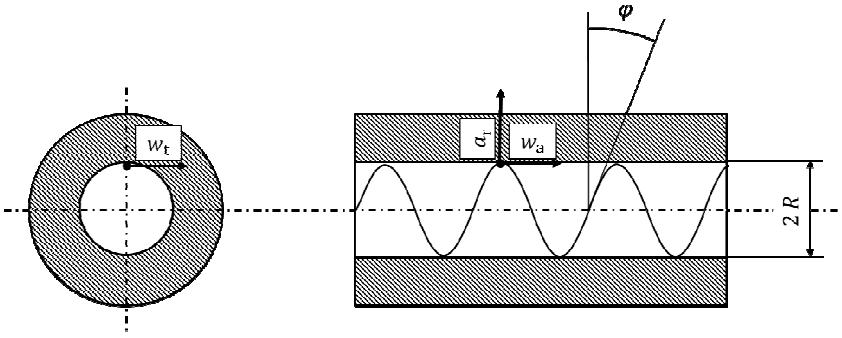

Figure 2: Ideal twisted flow with velocity and acceleration vectors. Sinusoidal line in pipe cut shows flow line of a fluidic particle next to pipe wall. No display of twist generating geometry, no-slip condition

To detect the form of the flow, flow pattern maps are in use. These maps have to be selected according to the actual pipe dimension and the pipe set up (fins, i.e.) (Rollmann, 2011). With fully wetted walls an increase of heat flux is predicted but not considered in the Yagov-model. With the Yagov model the critical heat flux of known fluids can be calculated at given radial accelerations. Taking R404A as fluid, rising of the critical heat flux by factor two to three compared to non-twisted flow is possible, as shown in figure 3. To verify the Yagov model the well-known model of Zuber (1959) to calculate critical heat flux was used for comparison as well.

The present work focusses on the experimental analysis of twisted flow in spot evaporators and the comparison to both, the Zuber and the Yagov models. Two different methods of generating the flow will be used and compared to each other. Refrigerant R404A[1] is chosen because of the reachable low temperatures of evaporation at pressures between 0.1 to 0.5 MPa. The electrical isolation in linear motors has very low heat conductivity so low evaporation temperatures of the coolant are helpful to reach processable heat transfer rates.

[1] To replace R404A (GWP = 3900) experiments using R32 (GWP = 675) are in progress

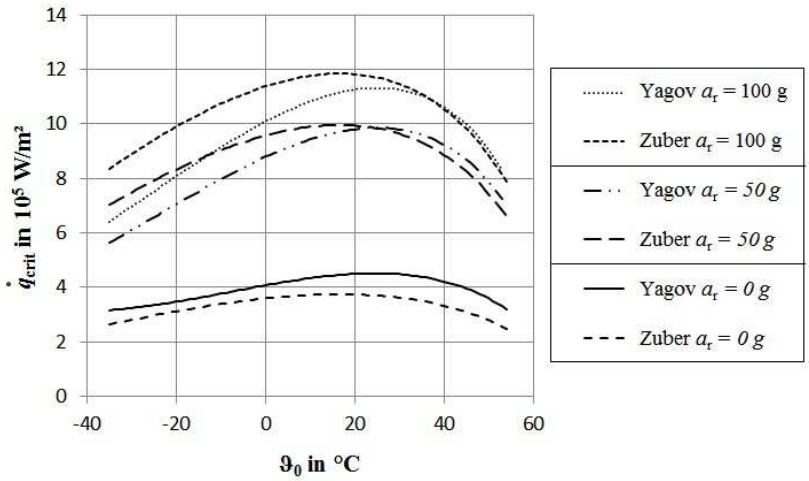

Figure 3: Critical heat flux of R404A in twisted flow spot calculated with the Yagov and the Zuber model at different radial accelerations.

2. EXPERIMENTAL SETUP

2.1 Flow loop

Figure 4 shows a schematic diagram of the test setup used to investigate heat transfer at high heat fluxes. The test setup consists of a hermetically sealed circuit with a continuously working compressor, a condenser, the test section assembly in which the refrigerant evaporates, several valves to control the flow, a mass flow meter and instrumentation. Subcooling is adjusted by a separate closed loop with a heater and an evaporator linked to the test loop through a heat exchanger. The water-heated post-evaporator is installed to make sure that only gaseous, superheated refrigerant is sucked by the compressor. The thermostatic expansion valve is used to regulate the evaporation pressure. The phase of the refrigerant can be checked by sight glasses installed at several positions.

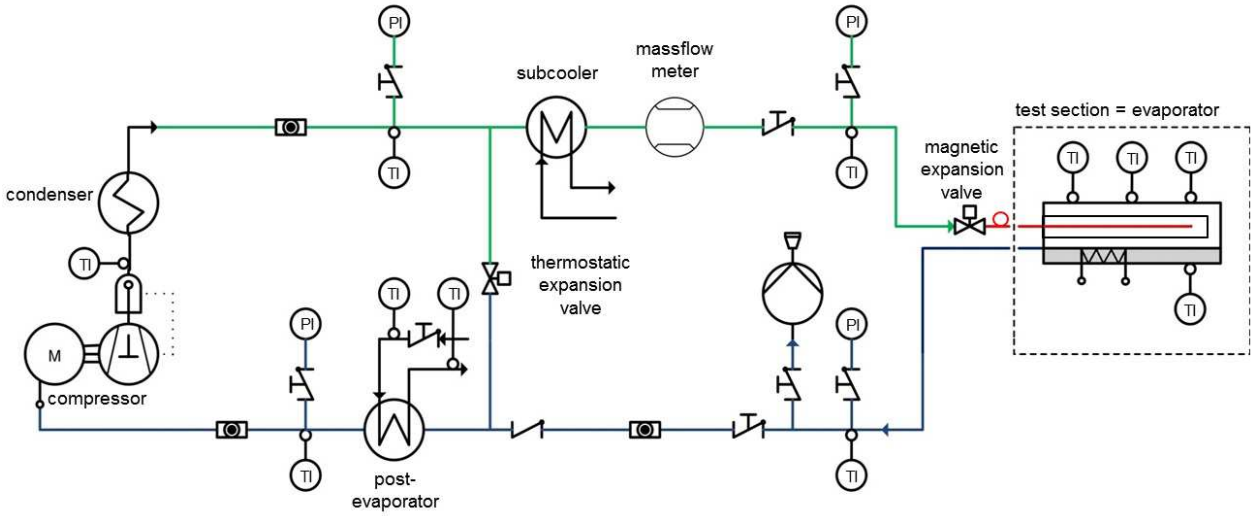

Figure 4: Experimental setup for heat transfer investigation at high heat fluxes

According to the considerations in chapter one, two different twist flow generating geometries have been produced. The first one is contains wire inserts, the second one contains a screw-inlet. As blank for the wire insert a tension spring has been used. Outer diameter of the spring was 5.2 mm above inner diameter of the blind hole of the spot evaporator. Using the reset force of the spring it could be assumed, that there was no gap between the spring and the wall of the blind hole. Visual inspection confirmed this assumption. The outer diameter of the screw for the second inlet was chosen 0.1 mm larger than inner diameter of the blind hole. Screwing the screw into the blind hole little

thread forming takes place and forms a winding. The winding has two functionalities. First is the fixing of the screw in the blind hole, second is a prevention of gap between screw and blind hole wall. Visual inspection confirms the close seat of the screw. To place the capillary tube inside the screw a hole was processed inside the screw using drilling EDM technology.

2.2 Data acquisition and uncertainties

12 temperature and 5 pressure sensors are installed in the experimental setup as shown in figure 4. Each reported measurement is an arithmetic mean of approximately 1200 points obtained over 10 minutes of steady-state conditions. The electrical power to the AC heating elements within the test section is measured using a combined voltage and current measurement system which has an uncertainty of 0.5 % of full scale. The refrigerant mass flow is measured with a Coriolis-type mass flow meter with an uncertainty of 0.1 % of the reading within the measurement range of 0 to 0.025 kg/s. Pressures at different points in the loop are measured using absolute pressure transducers with a range of 3.5 MPa and an uncertainty of 0.05 % of full scale. All temperatures are measured using calibrated J-type thermocouples with an uncertainty of ±0.1 K. Because of the dynamic of the process more accurate thermocouples are not used.

2.3 Experimental procedure

Critical heat flux depends on various parameters. Most spread measuring method was first introduced by Bonn *et al*. (1980). Using this method heating energy will be increased incrementally until critical heat flux is reached. The increment mostly depends on the materials used in the experimental setup and the distance between actual heating energy and predicted heating energy at the critical heat flux point. Characteristic for reaching critical heat flux is a sudden increase of wall temperature inside the test section (figure 5, 2100 s). This behavior has already been observed and described (Knipping, 2012).

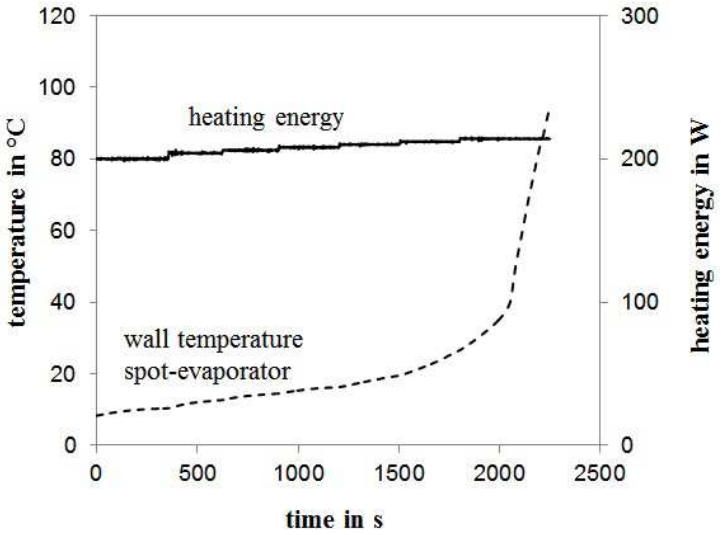

Figure 5: Characteristic graph (experimental data) to investigate critical heat flux

The increase of wall temperature can reach burn out state. To prevent this event heating is switched off after the wall temperature reaches 115 °C. Measurement data at increasing moment is stored and used to calculate critical heat flux. With known heated area and measured energy input critical heat flux can be calculated. Two measurement runs have been performed per measuring point. Mass flow was adjusted by varying high pressure of the refrigerant cycle. Subcooling was varied between 6 to 8 K, evaporating pressures between 0.2 and 0.3 MPa and mass flows between 0.001 to 0.002 kg/s. Mass flow increments have been 0.00015 kg/s. Each result with twisted flow was compared to reference measuring without twisted flow.

3. EXPERIMENTAL RESULTS

In order to identify the influence of mass flow on different twist generating geometries a curve was constructed from the measurement data as shown in figure 6. Heat flux has been calculated at given heating energy flows as well and is displayed on the second axis. Compared to Knipping *et al.* (2012) who used critical heat flux over mass flux as graph other form of presentation was used. This is necessary, because the twist generating geometry occurs a reduction of flow diameter and flow vectors don't show in axial direction of the tube. To display actual mass flux the orthogonal directed mass flux vector to the flow direction has to be calculated simultaneously at any point.

All measurement data has been compared to theoretical cooling capacities. Theoretical cooling capacity can be calculated using the enthalpy difference from entering the evaporator to full evaporation at the dew line in lg-p,h-diagram.

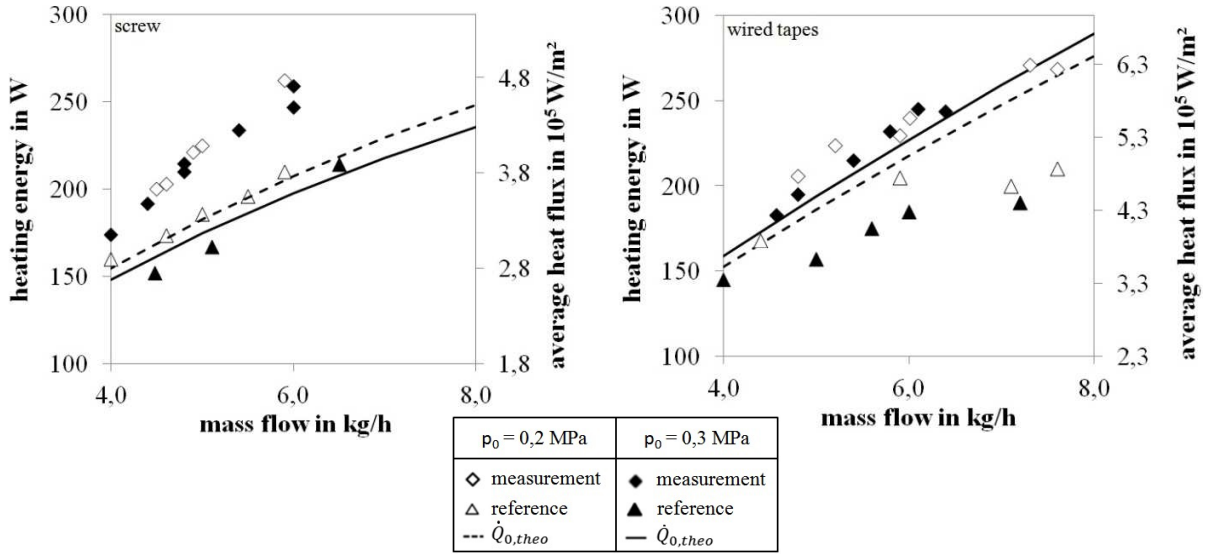

Figure 6: Measurement results and maximum transferrable heat using screws (left) and wired tapes (right) as twist generating geometries

The diagrams show, that reference measurements, which were generated at spot evaporators without twisted flow nearly match the theoretically calculated maximum transferrable energy $\dot{Q}_{0,\mathrm{theo}}$. This means, that all refrigerant is evaporated within the spot evaporator. All measurement points below the theoretical line mean, that not all refrigerant is evaporated in the evaporator. Without twisted flow fluidic, non-evaporated refrigerant is detected at the outlet of the evaporator. The refrigerant could not be evaporated because of the Leidenfrost-effect. It is also shown, that using twisted flow within the spot evaporators, all measurement data is above the theoretical line. This means, that refrigerant is superheated at the end of the twisted spot evaporator.

It is also shown in the diagrams, that at given mass flows $\dot{Q}_{0,\mathrm{theo}}$ is about 20 % higher with the wired tapes than with the screw inlet. This is because of the reduction of the flow diameter using a screw compared to using twisted tapes. Evaporation pressure has no significant influence within the displayed regions.

Using correlations between reference measure without twisted flow and twisted flow evaporators a percentile improvement of maximum transferable energy over mass flow can be displayed (figure 7). The graph shows, that under twisted conditions maximum transferrable heat mainly depends on mass flow. This is expected according to the investigations of Knipping et al. (2012) and Kim et al. (2005). At all mass flows maximum transferrable energy is significantly higher within the twisted spot evaporators compared to evaporators without twist generating geometry.

It is shown, that at low mass flows twisted tapes and screws nearly match in their ability to improve maximum transferrable energies. If mass flows are higher than 5 kg/h twisted tapes have better improvement rates than screws of about 2 - 3 % within the investigated region of mass flows. Higher mass flows could not be investigated due to pressure losses within the capillary tube. Bigger capillary tubes could not be used due to volumetrically limitations in applications of the spot evaporators.

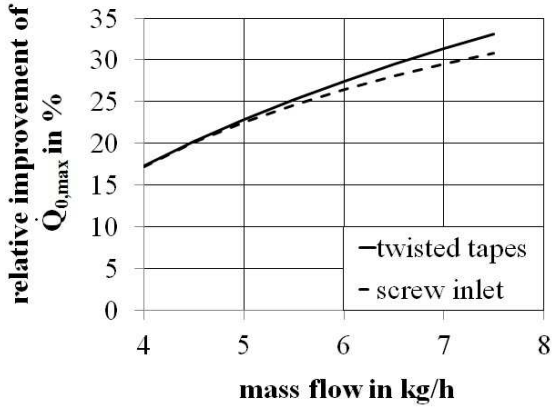

Figure 7: Relative improvement of maximum transferrable heat as a function of mass flow

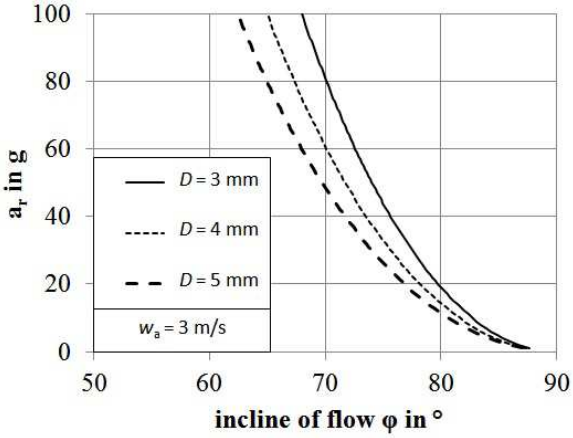

Figure 8: radial acceleration of the fluid as function of incline of flow

Using axial flow velocity of 3 ms^{-1} radial acceleration can be calculated using the model of Chang *et al*. (2006) as shown in Figure 8 for different diameters of the spot evaporator. Experiments have been processed using a spot evaporator with an inner diameter of 5 mm. Using Figure 3 at processed boiling temperatures it is shown that all measurement points are below the expected range of critical heat flux compared to the Zuber and Yagov models. One reason for this could be the high value of superheating. Figure 9 shows superheating of the refrigerant at different mass flows. As shown in the graph, superheat can reach up to 40 K. As mentioned before, mass flow could not be raised due to geometrical reasons. The difference in measured critical heat flux compared to the models of Zuber and Yagov is assumed to be relied on decrease of wetted surface within the spot evaporator. The reduction of wetted surface within the spot evaporator due to fully evaporated refrigerant leads to a flow of heat to wetted surfaces according to the second law of thermodynamics. Heat transfer coefficients are supposed to be much higher within wetted regions of the spot evaporator than in regions without wetted surface. The actual critical heat flux in the wetted part of the evaporator is then even higher than the displayed in the figures of this paper.

It is also displayed, that superheating of the refrigerant is much higher when using screws compared to wired tapes. The reason for this could probably found within the geometry of the testing area. The screw forces all liquid refrigerant into twisted flow. Twisted tapes have a little space between the capillary tube and the twist generating geometry. This gap gives the refrigerant the possibility to flow annually along the capillary tube and be evaporated later in the test section. Thus the wetted area is bigger compared to the screw inlet which leads to lower critical heat fluxes.

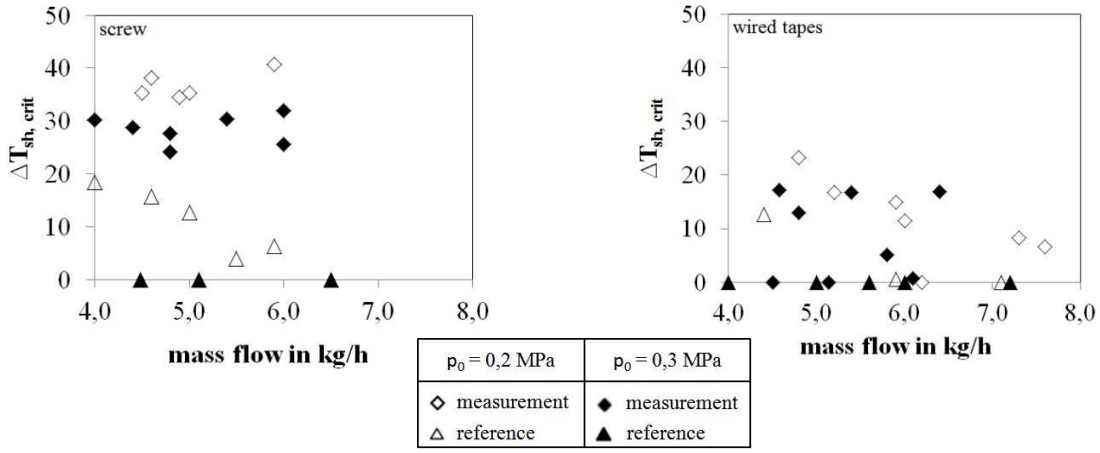

Figure 9: Superheat of refrigerant inside evaporator using screws (left) and wired tapes (right) as twist generation geometry

4. CONCLUSIONS

Spot evaporators are used in various components of processing technologies such as linear motors, plastic parts or milling tools. To improve the capacity of spot evaporators twisted flow has to be generated. Two methods of generating the twist have been observed. One with wired inserts, second with screw as twist generating geometry. Mass flows have been varied between 4.0 and 7.5 kg/h. R404A has been used as refrigerant.

It was shown that mass flow has strong influence on critical heat flux. Spot evaporators can be enhanced using twisted flow geometries. The maximum transferred heat can be raised about 30 % compared to spot evaporators without twist generation elements. Superheating of the refrigerant was up to 40K. The zone of superheating varies with used mass flows. Thus critical heat flux is much higher, than calculated.

NOMENCLATURE

EDM	electrical discharge machining	(-)	R	pipe diameter	(m)
PI	pressure transducer	(-)	$\Delta T_{\mathrm{sh,crit}}$	superheat of refrigerant	(K)
TI	temperature transducer	(-)	t	time	(s)
M	motor	(-)	w_{a}	axial flow velocity	(m/s)
a_{r}	radial acceleration	(m/s²)	w_{t}	tangential flow velocity	(m/s)
D_{SV}	diameter of the spot evaporator	(m)	ϑ_0	boiling temperature	(°C)
g	gravitational acceleration	(m/s²)	$\dot{m}_{\mathrm{R\_in}}$	incoming mass flow	(kg/s)
$\dot{m}$	mass flow	(kg/s)	$\dot{m}_{\mathrm{R\_out}}$	outgoing mass flow	(kg/s)
p_0	evaporation pressure	(MPa)	β	spraying angle	(°)
$\dot{Q}_0$	cooling capacity	(W)	L_{SV}	length of spot evaporator	(m)
$\dot{Q}_{0,\mathrm{theo}}$	theoretical cooling capacity	(W)	$\emptyset D_{\mathrm{K}}$	diameter of capillary tube	(m)
$\dot{q}$	average heat flux	(W/m²)	L_{KW}	distance surface-nozzle	(m)
φ	incline of flow	(°)	$\dot{Q}_{0,\mathrm{max}}$	maximum cooling capacity	(W)

REFERENCES

Ausderau, D., 2004: Polysolenid-Linearmotor mit genutetem Stator. PhD-Thesis ETH Zürich

Bogdanic, L., 2012: Two-Phase structure underneath a water jet impinging on a hot surface; PhD-Thesis TU Berlin

Bonn, W., Krebs R., Steiner D., 1980: Kritische Wärmestromdichte bei der Zweiphasenströmung von Stickstoff im waagrechten Rohr bei Drücken bis zum kritischen Druck. In: Wärme- und Stoffübertragung 14 p. 31 – 42

Celata, G.P.; Cumo, M., 1992: Burnout at high heat fluxes. In: Wärme- und Stoffübertragung 27, p. 233 - 244

Chang, S.H. 2006: Critical Heat Flux Enhancement. In: Nuclear Engineering and Technology 38, p. 753 – 761

Denkena, B., und Tönshoff, H.K., 2011: Spanen Grundlagen, Springer-Verlag, Berlin

Ganz, M., 2012: Entwicklung und Erprobung eines Verdampfers für Linearmotoren. Masterthesis Hochschule Karlsruhe – Technik und Wirtschaft

Hein, G., 2011: Werkzeugmaschinen-Produktion. In: Die deutsche Werkzeugmaschinenindustrie im Jahr 2010, Verein Deutscher Werkzeugmaschinenfabriken e.V. (VDW)

Hong, S. Y.; Ding, Y., 2001: Cooling approaches and cutting temperatures in cryogenic machining of Ti–6Al–4V. International Journal of Machine Tools and Manufacture. p. 1417-1437

Karaguezel, U.; Olgun, U.; Uysal, E.; Budek, E.; Bakkal, M., 2013: High Performance Turning of High temperature Alloys on multi-tasking machine Tools. Proceedings of the 4th Machining Innovations Conference, Hannover

Kim, C. H., Bang, I.C.; Chang, S.H., 2005.: Critical heat flux performance for flow boiling of R-134a in vertical uniformly heated smooth tube and rifled tubes. In: International Journal of Heat and Mass Transfer 48 p. 2868 – 2877

Knipping, K.; Arnemann, M.; Hesse, U.; Humpfer, F.; Ganz, M., 2012: Forced bulk boiling at high heat fluxes. Purdue conference proceedings 2012, Paper No. 2586

Marcinichen, J.B.; Olivier, J.: Lamaison, N.; Thome, J.R., 2013: Advances in Electronics Cooling, Heat Transfer Engineering, 34:5-6, p.434-446

Milnes, J., 2010: Computational Modelling of the HyperVapotron Cooling Technique for Nuclear Fusion Applications; PhD-Thesis Cranfield University

Mirghani, I.; Ahmeda, A. F.; Ismail, Y.A.; Abakr, A.K.M.; Nurul, A., 2007: Effectiveness of cryogenic machining with modified tool holder Journal of Materials Processing Technology 185, p. 91-96

Pusavec, F.; Hamdi, H.; Kopac, J.; Jawahir, I.S., 2010: Surface integrity in cryogenic machining of nickel based alloy - Inconel 718. Journal of Materials Processing Technology. p. 773-783

Rollmann, P. ; Spindler, K., 2011: Strömungsformen und Strömungsformkarten für die Verdampfung in horizontalen Rohren. DKV-Tagung 2011, Aachen, AA II.1

Seiler-Marie, N., 2004: Transition boiling at jet impingement. In: International Journal of Heat and Mass Transfer 47, p. 5059 – 5070

VDI Gesellschaft, 2013: VDI-Wärmeatlas. 10., bearb. und erw. Aufl. Berlin 2006

Webb, R. L., 1994: Principles of enhanced heat transfer. New York: Wiley

Weck, C.M.; Brecher, M., 2006: Werkzeugmaschinen 3: Mechatronische Systeme, Vorschubantriebe, Prozessdiagnose. 6., neu bearbeitete Auflage, Springer Verlag Berlin

Weinert, K., 2007: Spanende Fertigung – Prozesse, Innovationen, Werkstoffe. 4.Ausgabe; Vulkan Verlag (2005)

Wessels, Torsten. „Bohren in Titan- und Nickelbasislegierungen.“ Braunschweig: Institut für Werkzeugmaschinen und Fertigungstechnik der Technischen Universität

Yagov, V., 1988: A physical model and calculation formular for critical heat fluxes with nucleate pool boiling of liquids. In: Termal Engineering 35, No. 6, p. 333 – 339

Yagov, V., 2005: Heat transfer and crisis in swirl flow boiling. In: Experimental Thermal and Fluid Sciences 29 p. 871 – 883

Zuber, N., 1959: Hydrodynamic aspects of boiling heat transfer. Dissertation University of California. Atomic Energy Comission Report AECU-4439 Los Angeles